Development of small form factor packaged single-mode semiconductor laser for spectroscopic applications at 689nm

Seán P. Ó Dúill,[1,*] Richard Phelan,[2] Michael Gleeson,[2] Diarmuid Byrne,[2] John O'Carroll,[2] Neal Boylan,[2] Marta Nawrocka,[2] Emma Lambkin,[2] Kevin Carney, [2] Lina Maigyte,[2] Rob Lennox,[2] Jim Somers, [2] Brian Kelly,[2] Matthew J. Bartlow,[3] David B. Foote,[3] Adam T. Heiniger,[3] Chris Haimberger,[3] Moritz von Sivers,[4] Alexander Bachmann,[4] Florian Löffler[4], N. Pavlov,[5] John D. Jost,[5] and Liam P. Barry[1]

1) Radio and Optics Communications Laboratory, School of Electronic Engineering, Dublin City University, Glasnevin, Dublin 9, Ireland
2) Eblana Photonics West Pier Business Campus, 3 Old Dunleary Rd, Dún Laoghaire, Dublin, A96 A621, Ireland
3) TOPTICA Photonics, Inc., 1120 Pittsford Victor Rd, Pittsford, NY 14534, USA
4) TOPTICA Photonics AG, Lochhamer Schlag 19, D-82166 Graefelfing, Germany
5) Enlightra, Rue de Lausanne 64, 1020 Renens, Switzerland

* Corresponding author email sean.oduill@dcu.ie

Abstract—We report on the development of a compact packaged semiconductor laser capable of spectroscopy applications at 689 nm. The key component is an optical isolator that is small enough to fit inside a package that is compatible with standard 14-pin butterfly packages. We present a threshold current of 33 mA, a forward voltage of 2.5 V at 50 mA, long term reliability study for over 12,500 hours, a relative intensity noise below -145 dBc/Hz, and a linewidth of 2 MHz. The relative intensity noise and the frequency noise spectra verify continuous-wave lasing and frequency stability of the packaged laser.

Index Terms—Semiconductor lasers, laser packaging, spectroscopy, noise, intensity noise, frequency noise

I. INTRODUCTION

The need for smaller form factor and more spectrally precise lasers is a basic demand across every market where lasers are a key technology. The key parameter for stable lasers is the linewidth and this is extremely important for sensitive sensing applications such as advance timekeeping [1], LIDAR [1,3], and atomic cooling [4] to name a few. Many of these sensing applications also require wavelengths operating around 689nm [4]. There are limited commercial options for compact low linewidth single mode lasers around 689 nm [5] and one of the major challenges is the lack of micro-optical isolators at this wavelength which can be inserted in a 14-pin butterfly module. In recent years, single-mode semiconductor lasers emitting in the red have been fabricated using discrete mode (DM) waveguide design [6] distributed Bragg reflector [7] and surface grating distributed feedback ridge waveguides [8, 9]. While the lasing active material can be band-gap engineered by selection of the InGaP material and appropriate grating fabrication can ensure operation at the desired wavelength [6,7], the usefulness of the device depends on creating a single wavelength emission which is not made unstable by back reflections from extraneous parts of the interconnecting optical circuitry. These back reflections typically cause the laser output to have significantly increased linewidth, to become unstable, pulsate or introduce wavelength hopping. All these effects significantly reduce the usefulness of the laser in sensing-based applications.

In this paper we report on a stable, single-mode (both transverse and longitudinal), semiconductor laser packaged in a small-form factor 14-pin butterfly package operating at 689nm wavelength with fibre coupled output power of ~1 mW. The laser is based on a DM waveguide design [6] that defines the emission wavelength, the simplified schematic is shown in Fig. 1(b). Key to achieving stable performance is the co-packaged inclusion of a micro-optical isolator within the butterfly package that eliminates back reflections to the laser from the connected optical circuitry. Two packaged lasers are investigated and demonstrate similar performance with threshold currents of 33 mA, forward diode voltage of less than 2.5V, relative intensity noise (RIN) below -145 dBc/Hz, and a linewidth of ~2 MHz at 80 mA bias. Two techniques are used to measure the laser linewidth; the delayed self-heterodyne technique and the β-line cutoff method [10] where we heterodyne both lasers to measure the linewidth using the frequency noise (FN) spectral density [11].

This paper is organised as follows, in Section II we describe the laser and the packaging with special consideration given to the optical isolator and we present standard emission spectra and light-current-voltage (L-I-V) curves. In Section III we report on dynamic measurements to verify the stability of the laser emission from the package, namely RIN and linewidth including the β-line separation.

II. LASER and PACKAGING

The laser epitaxial structure was grown on 75mm diameter Si-doped GaAs substrates in a metal-organic vapour-phase epitaxy reactor at low pressure. The multiple quantum well active structure consisted of four compressively strained 10nm-thick GaInP quantum wells and three lattice-matched 7nm thick $(Al_{0.3}Ga_{0.7})_{0.51}In_{0.49}P$ barriers, sandwiched between two 40 nm-thick separate confinement guide layers. The 2.5μm thick upper and lower cladding material is $(Al_{0.7}Ga_{0.3})_{0.51}In_{0.49}P$ and the p-cladding is followed by a 250nm thick, highly p-doped, GaAs contact layer. A simplified schematic is shown in Fig. 1(a). More detailed information on the laser design can be found in [6].

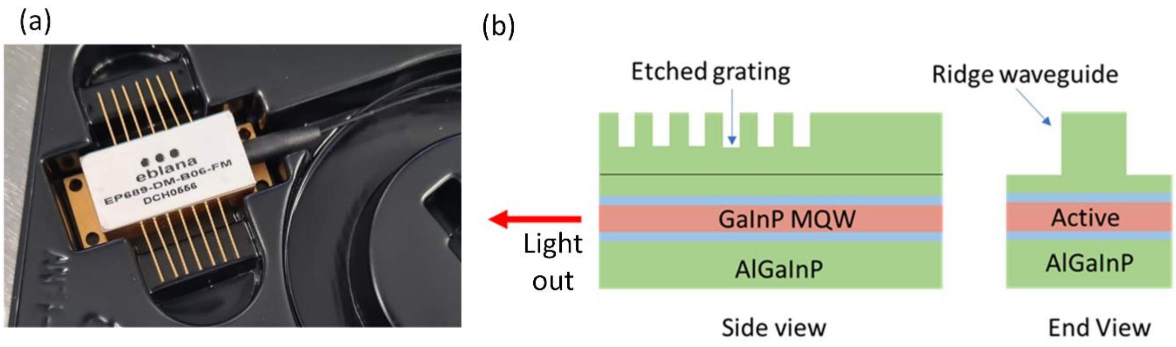

Fig. 1 (a) Simplified schematic of the DM laser [6]. (b) Picture of 14-pin butterfly module.

Semiconductor lasers need to be co-packaged with electronics and light coupling optics for practical use within lightwave systems [1-4]. A key component in any laser package is an optical isolator that forbids light travel back towards the laser because single longitudinal mode lasers suffer from intensity and frequency instability when subjected to back reflections. Optical isolators consist of a Faraday polarization rotator in a strong magnetic field, placed between two polarizers. Over propagation distance L in a constant magnetic field B, the Faraday rotator rotates linear polarization by an angle $\vartheta = VBL$, where V is the Verdet constant of the material. For visible wavelengths, terbium gallium garnet (TGG) crystals are frequently used as the Faraday rotator. At these wavelengths, TGG has high transmission and high Verdet constant (>100 rad/T/m) [12]. TGG can be placed in neodymium iron boron magnets to create an isolator with high performance at low cost. Such isolators range in size from 10 cm^3 to 100 cm^3 depending on wavelength and beam diameter. Unfortunately, TGG isolators are unfeasible to place inside a small butterfly package. Very small optical isolators based on bismuth-substituted rare earth iron garnet single crystals are frequently used in the near-infrared, but this material suffers from high absorption loss at wavelengths below approximately 1000 nm [13]. Cadmium manganese telluride Faraday rotators have been developed in recent years with very high Verdet constants (>1000 rad/T/m) and low losses at wavelengths above 600 nm. With such materials, it is possible to fabricate an isolator at 689 nm that is < 1 cm^3 in volume with high extinction and low losses [14]. Such an isolator is used in this work and had a transmission of 52% and optical isolation of 34.5dB at 689nm. In order to accommodate these Cadmium manganese telluride mini free space optical isolators into a temperature-controlled module, a non-standard 14-pin butterfly package was designed and manufactured with dimensions $L_p \times W_p \times H_p$ of 39.1 x 17.7 x 9.7 mm, a photograph of which is given in Fig. 1(b). In comparison a standard 14-pin butterfly package would have the following dimensions $L_p \times W_p \times H_p$ of 30 x 15.2 x 7.7 mm. The length of the butterfly package module was chosen to allow for the insertion of a single-stage isolator with 34.5 dB isolation; increasing the isolation would require increasing the length of the entire package. The chosen isolator is therefore a compromise between the overall isolation level sufficient to stop deleterious back reflections and for the laser system to fit within a small form factor 14-pin butterfly package. Inside this hermetically sealed module, the isolator is positioned between two lenses which are antireflection coated at 689nm in order to reduce optical reflections and scattering effects. The first lens acts to collimate the output from the laser diode, to match the numerical aperture of the isolator. The light then propagates through the isolator to the second lens, which focuses the output light into a low attenuation narrow core polarisation-maintaining single mode fibre. The laser temperature is stabilised through the use of a Thermo-Electric Cooler (TEC) and a thermistor placed adjacent to the laser diode. It must be noted that a fibre-coupled, external optical isolator was placed after the module fibre connector to provide extra isolation from the connected optical circuitry. The external isolator alone does not solve the issue of internal back reflections within the module that can create a pulsating laser output.

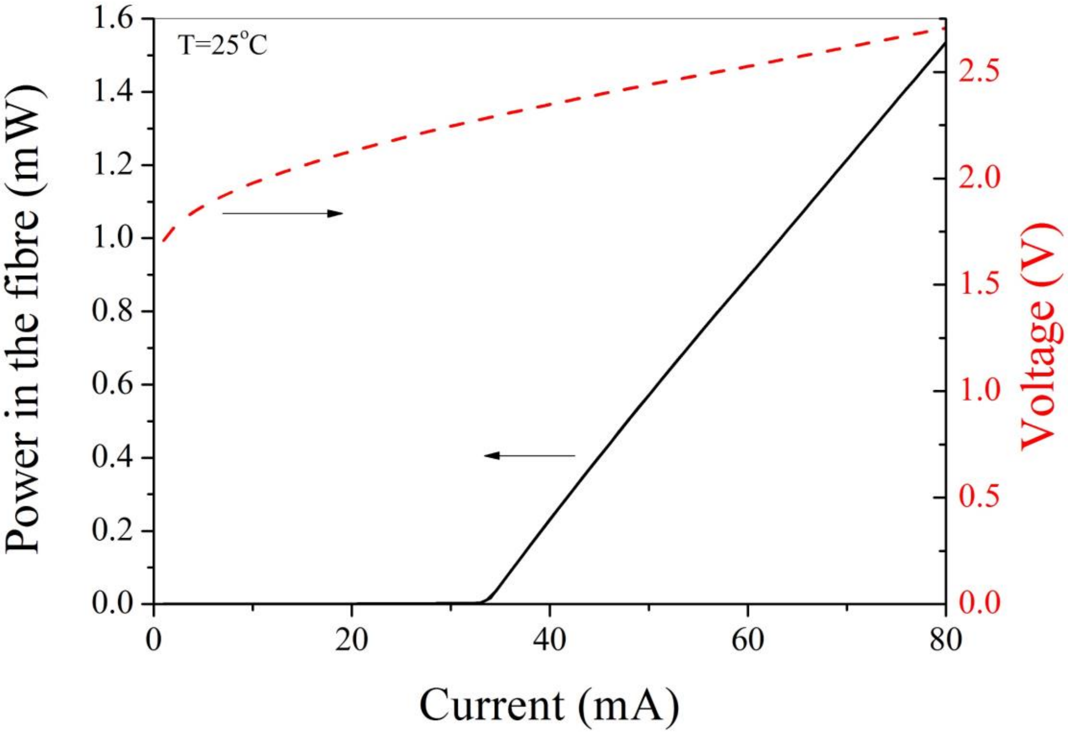

Fig. 2 Measured L-I-V curve of the butterfly packaged 689nm laser. The threshold current is about 33 mA, and the forward voltage is around 2.8 V at a forward bias of 80 mA.

The optical characteristics of the packaged 689nm laser were measured under CW bias conditionsFig. 2 plots the overlapped measurement of fibre coupled LIV characteristics at a chip temperature of 25 ˚C where the power was measured with a Si detector. The extracted threshold current was 33 mA and the slope efficiency from the emitting laser facet end of the optical fibre is 0.15 W/A. This corresponds to a 16% fibre coupling efficiency. The forward voltage is in the range from 1.75 V to 2.6V as the bias current is varied from 1 mA to 80 mA. The emission spectra of the device are also measured for currents of 50 mA and 80 mA and shown in Fig. 3 with the central peak at 688.6 nm and side mode suppression ratio of 45dB. This measurement is shown for operating conditions of bias current of 50 mA at 25 ˚C. We performed lifetime testing on a similar 689nm laser chip mounted on a transistor outline (TO39) header (without the isolator and fibre coupling optics) which contained TEC and thermistor and the power from the facet was measured on a large area Si detector. The temperature of the laser was controlled to within 2mK. The emission power was measured over 12,500 hours and the results are presented in Fig. 4 showing a constant output power of ~6 mW with no degradation in power observed over the duration of the test. The outliers where the power drops are interruptions of the data acquisition due to maintenance issues.

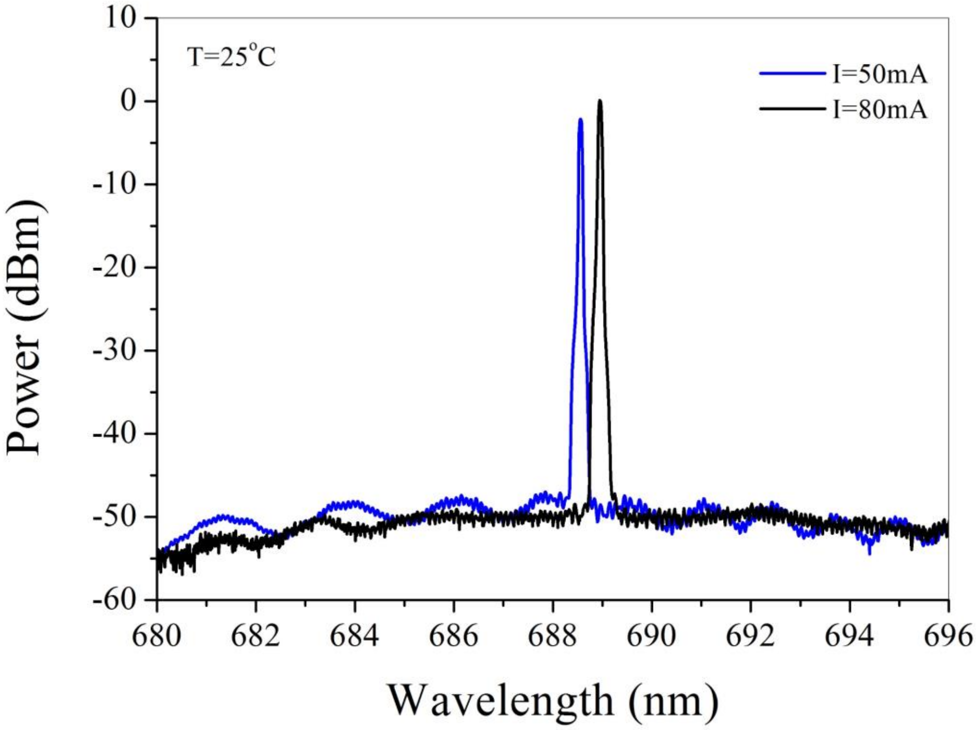

Fig. 3 Measured optical spectrum of the device, showing a single longitudinal mode operating at 688.3 nm (50 mA) and 688.6 nm (80 mA). The side-mode suppression exceeds 45 dB

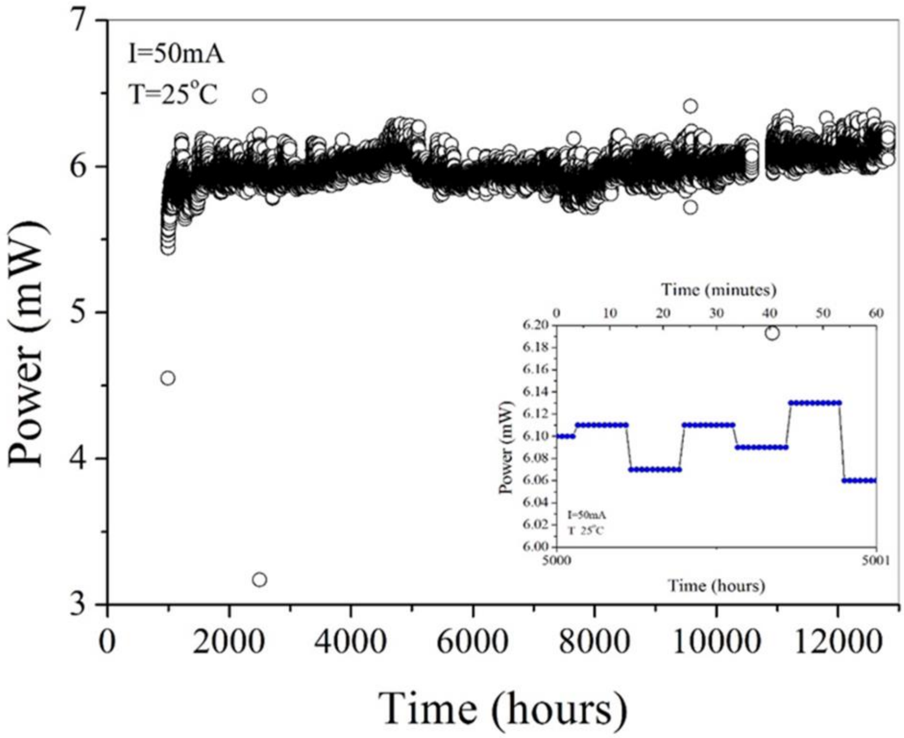

Fig. 4 Aging time dependence on the operating power at a fixed bias current of 50mA and temperature of 25°C for >12000 hours. Note, the device used to obtain this measurement was a similar laser diode except mounted on a TO39 header without isolator and coupling fibre optics, hence the reading of 6 mW at 50 mA bias current. The inset shows the power fluctuations over a 1 hour interval.

III. STABILITY MEASUREMENTS

To verify the CW stability of the packaged laser we perform the following measurements: firstly, we measure the laser RIN, then we measure the delayed self-heterodyne (DSH) beat spectrum and FN power spectral density (PSD) spectrum. For stable single-mode behaviour the following conditions should be met: a single peak in the RIN curve, a Lorentzian shaped DSH spectrum and a flat FM-noise curve. A single peak in the RIN curve notes the absence of self-pulsation; a detectable Lorentzian spectrum from DSH spectrum measurement implies wavelength stability over the duration of the DSH measurement which requires about five minutes to take 100 spectral averages; and a flat FM-noise curve underscores the Lorentzian line broadening in the absence of any external feedback.

The RIN setup is based on the standard RIN measurement [15]. The photodiode has a bandwidth of 30 GHz and we report a measured responsivity of 0.1 A/W at 688 nm, which suffices for these measurements. The RIN measurement was taken at two bias currents of 50 mA and 80 mA and the

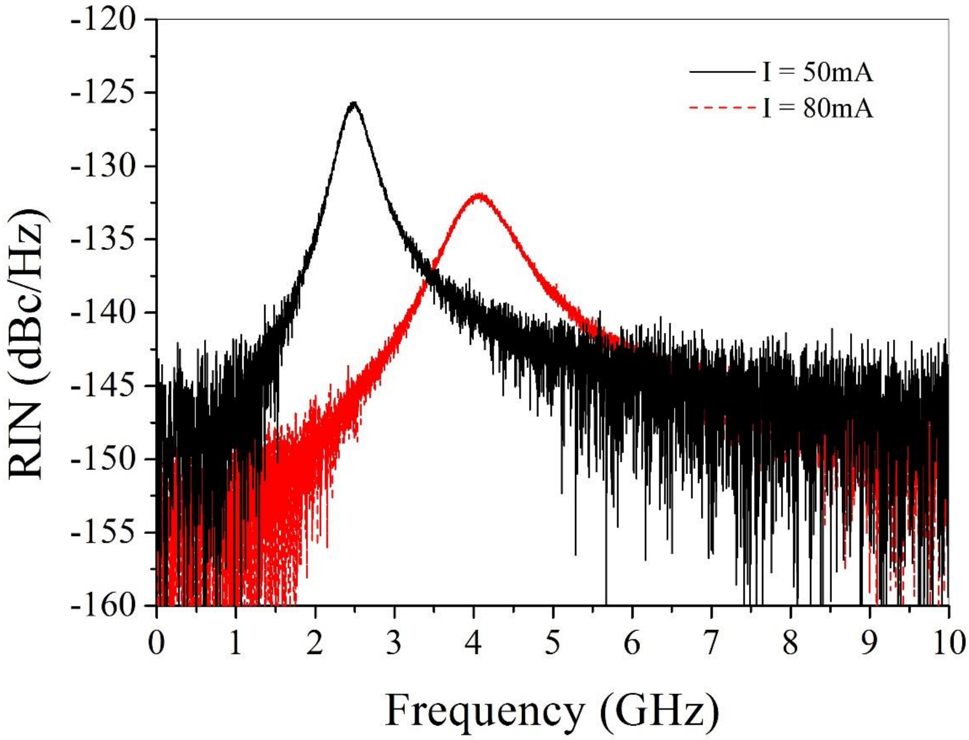

Fig. 5 Measured RIN curve of the light output from the laser at bias currents of 50 mA (black) and 80mA

results are shown in Fig. 5. The RIN at low frequencies is below -145 dBc/Hz with peaks occurring at relaxation oscillation frequencies of 2.6 GHz and 4 GHz for 50 mA and 80 mA bias respectively. There is clearly only one peak in the spectrum which implies that the laser is operating CW and not pulsating. Note that we were shot noise limited in estimating for the minimum because the DC photocurrent at the photodetector was ~around 0.1 mA; the shot noise limit to the RIN is given by $2q/\langle I_{PD}\rangle$ [15], for our case the shot noise limit is about -145 dBc for 50 mA bias case and -148 dBc at 80 mA bias case.

In order to verify the phase stability of the lasers, we measure the DSH spectrum from the laser. The DSH spectrum was measured in the standard manner [15] using a phase modulator and 1 km fibre

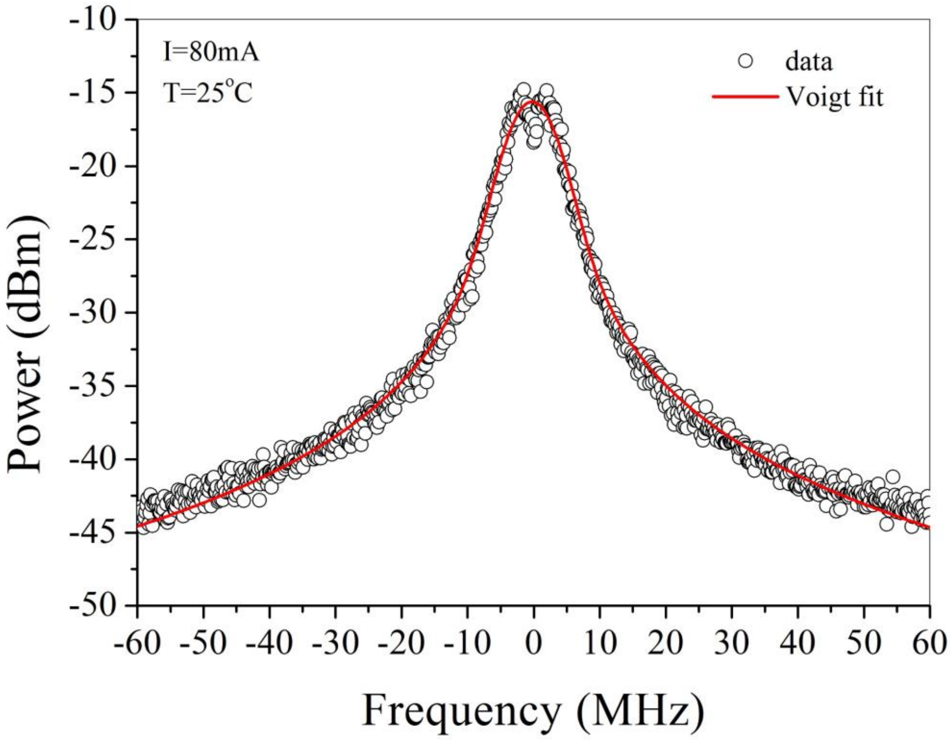

Fig. 6 Measured and Voigt-fitted DSH spectrum of the device, the extracted intrinsic Lorentzian linewidth is 1.4 MHz.

reel suitably designed to guide light at 689 nm in a single mode. The DSH spectrum is measured using an electrical spectrum analyser and the trace has been averaged one hundred times before fitting with a Voigt curve [16]. The results are shown in Fig. 6. The extracted intrinsic Lorentzian linewidth is 1.4 MHz from the Voigt curve fitting. The importance of averaging many scans is that multiple peaks will show up in the DSH spectrum of wavelength-unstable lasers [17]. Therefore we conclude that the packaged laser is operating stably in both power and wavelength.

The FN spectral density spectrum (SD) can be described by the following general relation [18-21]:

$$FN(f) = \frac{h_{-1}}{f^{\alpha}} + h_0 \quad (1)$$

The first term is for the *1/f* flicker noise which dominates the linewidth for most semiconductor laser diodes where *f* is the frequency, exponent α ($1< \alpha <2$), h_{-1} is a constant and the last term h_o is the white frequency or intrinsic noise. The FN PSD curve was measured by beating two similarly packaged 689nm lasers, capturing the beat using a digital storage oscilloscope and post-processing the beat signal to calculate the FN PSD which is shown in Fig 7. More details on this procedure are given in [22]. The FN approximation in (1) is fitted to the FN noise plot as shown in 7; and h_{-1}, α, and h_o are extracted to be 1×10^{-14}, 1.45 and 500000 Hz^2/Hz respectively for the 689nm laser.

The lasing linewidth is estimated from the measured FN spectrum utilizing the β-separation line method in [10,23]. The β-separation line is used to separate high and low modulation index areas in the FN PSD, which distinguishes contributions to the linewidth versus the wings of the lineshape [10]. In our calculation, the frequency noise is integrated from 10 , 20 and 50kHz out to the intersection with the β-separation line, yielding an integrated linewidth of 5, 3.2 and 1.8MHz for the various timescales. We also extract the white noise level directly proportional to intrinsic (Lorentzian) linewidth to be ~1.5MHz.

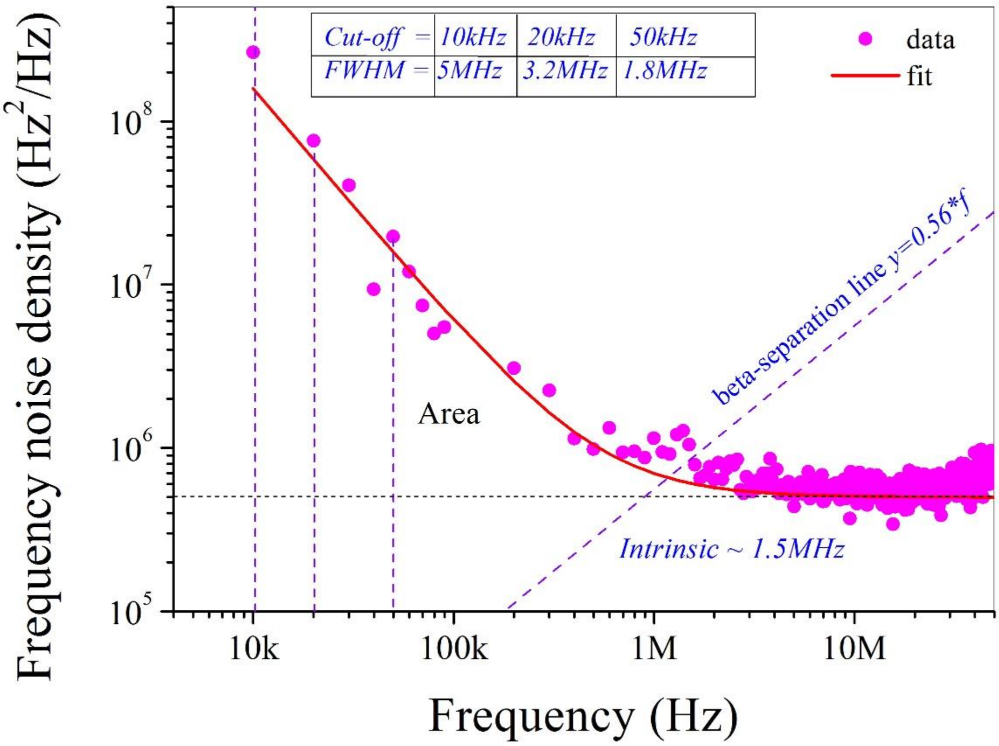

Fig. 7. Measured FN-noise spectral density from the beating between two similar 689nm DM devices. Linewidth at various timescales extracted using the β-separation line method. The measurement was performed at a bias current of 80 mA. The red line is a fitting to the curve described by Eq. (1).

Conclusion

We demonstrate for the first time a stable, small form-factor, lightweight, packaged semiconductor laser operating at 689 nm; and this packaged laser enables the use of such devices to create compact sensors in the 689nm window. The laser stability is enabled through the use of suitably small cadmium manganese telluride optical isolators and a customised 14-pin butterfly package that is compatible with 14-pin butterfly mounts. We show expected single-mode, single-wavelength operation and report the RIN and frequency noise measurements of the 689nm single wavelength AlGaInP laser diode.

Acknowledgement

This work was supported in part by the European Space Agency under Contract number 400012492018/NL/GLC/fk and Science Foundation Ireland through project 12/RC/2276_P2.

References

1. Z. L. Newman, V. Maurice, T. Drake, J. R. Stone, T. C. Briles, D. T. Spencer, C. Fredrick, Q. Li, D. Westly, B. R. Ilic, B. Shen, M.-G. Suh, K. Y. Yang, C. Johnson, D. M. S. Johnson, L. Hollberg, K.J. Vahala, K. Srinivasan, S. A. Diddams, J. Kitching, S. B. Papp, and M. T. Hummon," Architecture for the photonic integration of an optical atomic clock," Optica 6, No. 5, p.p. 680-685, 2019
2. P. A. Morton, C. Xiang, J. B. Khurgin, C. D. Morton, M. Tran, J. Peters, J. Guo, M. J. Morton, and J. E. Bowers, "Integrated Coherent Tunable Laser (ICTL) with ultra-wideband wavelength tuning and sub-100 Hz Lorentzian linewidth," IEEE J Lightwav Technol. 40, No. 6, p.p. 1802-1809, 2022
3. D. Bastos, P. P. Monteiro, A. S. R. Oliveira and M. V. Drummond, "An Overview of LiDAR Requirements and Techniques for Autonomous Driving," 2021 Telecoms Conference (ConfTELE), 2021, pp. 1-6, doi: 10.1109/ConfTELE50222.2021.9435580.
4. T. W. Hänsch, and A. Schawlow, "Cooling of gases by laser radiation," Optics Commun. 13, No. 1, p.p. 68-69, 1975
5. https://www.laserglow.com/product/D69-R-690-nm-Collimated-Diode-Laser-System (accessed 25/01/2023)
6. R. Phelan et al "InGaP/AlGaInP Quantum Well Discrete Mode Laser Diode Emitting at 689 nm" IEEE Photon. Technol. Lett., Vol. 30, No. 3, p.p. 235-237, 2018
7. C. Pyrlik, N. Goossen-Schmidt, A. Bawamia, J. Fricke, A. Knigge, A. Maaßdorf, M. Schiemangk, H. Wenzel, and A. Wicht, "High Power Distributed Bragg Reflector Lasers at 689.45 nm for Quantum Technology Applications," in IEEE Photonics Technology Letters, vol. 34, no. 13, pp. 679-682, 1 July1, 2022, doi: 10.1109/LPT.2021.3139433
8. G. Blume et al., "Narrow linewidth of 633-nm DBR ridge-waveguide lasers," IEEE Photon. Technol. Lett., vol. 25, no. 6, pp. 550–552, Feb. 1, 2013
9. J. Fricke, O. Brox, H. Wenzel, M. Matalla, P. Ressel, and A. Knigge, "Red-emitting distributed-feedback ridge-waveguide laser based on high-order surface grating," Electron. Lett., vol. 54, no. 9, pp. 582–583, May 2018.
10. G. Di Domenico, S. Schilt, and P. Thomann, "Simple approach to the relationship between laser frequency noise and laser line shape," Appl. Opt. 49, 4801-4807, 2010
11. K. Kikuchi, "Characterization of semiconductor-laser phase noise and estimation of bit-error rate performance with low-speed offline digital coherent receivers," Opt. Express 20(5), 5291–5302, 2012
12. D. Vojna, O. Slezák, A. Lucianetti, and T. Mocek, Applied Sciences 9, 3160 ,2019
13. G.B. Scott and D.E. Lacklison, IEEE Transactions on Magnetics 12, pp. 292-310, 1976
14. C. Nölleke P. Leisching, G. Blume, D. Jedrzejczyk, J. Pohl, D. Feise, A. Sahm, and K. Paschke, Proc. SPIE 10082, Solid State Lasers XXVI: Technology and Devices, 1008225 , 2017
15. G. Morthier, and V. Vankwikelberge, "Handbook of Distributed Feedback Laser Diodes," 2nd Ed. Artech House, ISBN 9781608077021, 2013
16. S. Spiessberger, M. Schiemangk, A. Wicht, H. Wenzel, O. Brox, and G. Erbert," Narrow Linewidth DFB Lasers Emitting Near a Wavelength of 1064 nm," IEEE/Optica J. Lightwav. Technol. 28, No. 6, p.p. 2611-2616, 2011
17. K. Petermann," External Optical Feedback Phenomena in Semiconductor Lasers," IEEE J. Sel Topics in Quantum Electron. 1, No. 2, p.p. 480-489
18. T. Okoshi, K. Kikuchi, and A. Nakayama, "Novel method for high resolution measurement of laser output spectrum," Electron. Lett. 16, 630-631, 1980

19. S. Kundermann, J. O'Carroll, D. Byrne, L. Maigyte, B.Kelly, R. Phelan, D. L. Boiko "Temperature and current dependence of 1/f frequency noise in narrow-linewidth discrete-mode lasers" Conference: European Semiconductor Laser Workshop - ESLW 2015
20. R. J. Fronen and L. K. J. Vandamme, "Low-frequency intensity noise in semiconductor lasers," IEEE J. Quantum Elect., vol. 24, pp. 724–736, 1988
21. K. Kikuchi, "Effect of 1/f-type FM noise on semiconductor-laser linewidth residual in high-power limit," IEEE J. Quantum Electron., vol. QE-25, p. 684, 1989
22. S. P. O'Duill, and L. P. Barry," High Precision Estimation of Laser FM-Noise Using RF Quadrature Demodulation Techniques," IEEE Access 10, p.p. 119875-119882, 2022
23. N. Bucalovic, V. Dolgovskiy, C. Schori, P. Thomann, G. Di Domenico, and S. Schilt, "Experimental validation of a simple approximation to determine the linewidth of a laser from its frequency noise spectrum," Appl. Opt. 51, 4582-4588, 2012